THE JOURNAL OF BIOLOGICAL CHEMISTRY VOL. 283, NO. 25, pp. 17020–17029, June 20, 2008
© 2008 by The American Society for Biochemistry and Molecular Biology, Inc. Printed in the U.S.A.

Endoplasmic Reticulum (ER) Chaperone Regulation and Survival of Cells Compensating for Deficiency in the ER Stress Response Kinase, PERK*

Received for publication, March 31, 2008 Published, JBC Papers in Press, April 21, 2008, DOI 10.1074/jbc.M802466200

Yukihiro Yamaguchi[‡], Dennis Larkin[‡], Roberto Lara-Lemus[‡], Jose Ramos-Castañeda[‡§], Ming Liu[‡], and Peter Arvan[‡1]

From the [‡]Division of Metabolism, Endocrinology & Diabetes, University of Michigan Medical Center, Ann Arbor, Michigan 48109 and the [§]Centro de Investigaciones sobre Enfermedades Infecciosas, 62580 Cuernavaca Morelos, Mexico

The activity of PERK, an endoplasmic reticulum (ER) transmembrane protein kinase, assists in an ER stress response designed to inhibit general protein synthesis while allowing up-regulated synthesis of selective proteins such as the ATF4 transcription factor. PERK null mice exhibit phenotypes that especially affect secretory cell types. Although embryonic fibroblasts from these mice are difficult to transfect with high efficiency, we have generated 293 cells stably expressing the PERK-K618A dominant negative mutant. 293/PERK-K618A cells, in response to ER stress: (*a*) do not properly inhibit general protein synthesis, (*b*) exhibit defective/delayed induction of ATF4 and BiP, and (*c*) exhibit exuberant splice activation of XBP1 and robust cleavage activation of ATF6, with abnormal regulation of calreticulin levels. The data suggest compensatory mechanisms allowing for cell survival in the absence of functional PERK. Interestingly, although induction of CHOP (a transcription factor implicated in apoptosis) is notably delayed after onset of ER stress, 293/PERK-K618A cells eventually produce CHOP at normal or even supranormal levels and exhibit increased apoptosis either in response to general ER stress or, more importantly, to specific misfolded secretory proteins.

A growing list of genetic diseases have been found to be accounted for by structural changes in secretory proteins that alter their folding and render them deficient for transport through the intracellular secretory pathway (1). Some of these diseases involve mere loss of function of the secreted protein (2), whereas others may be involve gain of toxic function to cells that attempt to produce them (3).

The endoplasmic reticulum (ER)[2] serves as the compartment initiating the biosynthesis of secretory proteins, providing a unique environment for folding and re-folding of nascent polypeptides, and for recognition and retention of secretory proteins that fail to fold to their native conformation (4) to direct their ultimate disposal via the ubiquitin-proteasome system (5) in a process known as ER-associated protein degradation (6). Preventing toxic accumulation of misfolded secretory proteins is vital for proper ER homeostasis (7, 8). When retained secretory proteins stress the capacity of ER quality control mechanisms for protein folding or disposal, the ER responds, using several distinct signaling systems to up-regulate the ER stress response (9).

The oldest and best recognized ER stress signaling pathway involves Ire1, an ER transmembrane protein conserved to the level of yeast (10). Upon ER stress activation, Ire1 becomes an active ribonuclease engaged in mRNA splicing to produce the active transcription factor XBP1 (11) (Hac1 in yeast (12)), which turns on many unfolded protein response genes (13), including those linked to ER-associated protein degradation (14). A second ER transmembrane protein involved in stress signaling is ATF6. Upon ER stress activation, the pro-ATF6 protein migrates from the ER to the Golgi complex where its cytosolic domain becomes proteolytically cleaved to an active transcription factor that is transported to the nucleus, similarly turning on many unfolded protein response genes (15), including XBP1 (16, 17).

A third ER transmembrane protein involved in stress signaling is PERK. PERK is one of four kinases whose cytosolic domain provides major input into the phosphorylation state of the eukaryotic initiation factor 2α (eIF2α)-Ser-51 (18), which in turn suppresses general protein synthesis (19), while allowing selected mRNAs (such as that encoding the ATF4 transcription factor (20, 21)) to be translated. PERK activity is analogous to that of certain cell surface receptors, using the extracytoplasmic domain for homodimerization, which in turn activates the cytosolic Ser-kinase domain (22, 23). Animals deficient for PERK, or mutant for Ser-51 of eIF2α, exhibit phenotypic abnormalities, especially in professional protein-secreting cell types (24). These observations raise the question of how cells deficient for PERK activity handle misfolded secretory proteins. Theoretically, such a question should be easily tested in mouse embryonic fibroblasts (MEFs) from PERK$^{-/-}$ mice transfected with cDNAs encoding specific mutant secretory proteins. However in practice,[3] we have found it extremely difficult to

* This work was supported, in whole or in part, by National Institutes of Health Grants R01 DK40344 and DK48280. The costs of publication of this article were defrayed in part by the payment of page charges. This article must therefore be hereby marked "*advertisement*" in accordance with 18 U.S.C. Section 1734 solely to indicate this fact.

[1] To whom correspondence should be addressed: Division of Metabolism, Endocrinology & Diabetes, University of Michigan Medical School, 5560 MSRB2, 1150 W. Medical Center Dr., Ann Arbor, MI 48109-0678. Tel.: 734-936-5505; Fax: 718-936-6684; E-mail: parvan@umich.edu.

[2] The abbreviations used are: ER, endoplasmic reticulum; PDI, protein disulfide isomerase; eIF2α, eukaryotic initiation factor 2α; MEF, mouse embryonic fibroblast; DMEM, Dulbecco's modified Eagle's medium; CMV, cytomegalovirus; Tg, thyroglobulin; ELISA, enzyme-linked immunosorbent assay; DAPI, 4′,6-diamidino-2-phenylindole; GFP, green fluorescent protein.

[3] Y. Yamaguchi, D. Larkin, R. Lara-Lemus, J. Ramos-Castañeda, M. Liu, and P. Arvan, unpublished data.

transfect these cells with reasonable efficiency. To circumvent this problem, we have employed an alternative approach in which 293 cells are stably transfected to overexpress PERK-K618A, a dominant-negative PERK mutant that blocks transphosphorylation and activation of the PERK kinase (19). These cells can be readily transfected with eukaryotic expression vectors, allowing us to study how PERK-deficient cells respond to the presence of misfolded secretory proteins within the ER compartment.

EXPERIMENTAL PROCEDURES

Antibodies—Rabbit anti-ATF6 was from Santa Cruz Biotechnology (#SC-22799 lot H-280) and used for Western blotting at a dilution of 1:100. Rabbit anti-ATF4 (also known as CREB-2, Santa Cruz Biotechnology #SC-200) and was used at 1:400 dilution. Mouse monoclonal antibody anti-CHOP (also known as GADD153, Santa Cruz Biotechnology #SC-7351) was used at a dilution of 1:40. Mouse monoclonal antibody anti-eIF2α total was from BIOSOURCE and used at a dilution of 1:100. Rabbit anti-phosphoSer-51 of eIF2α was also from BIOSOURCE and used at 1:100. Mouse monoclonal antibody anti-PDI was from Affinity BioReagents (#MA3-019) and used at 1:500. Rabbit anti-Myc was from ICL (#RMYC-45A-3) and used at a dilution of 1:5000). Chicken anti-calreticulin was used at a dilution of 1:2000). Rabbit anti-BiP (1:5000), rabbit anti-calnexin (1:2000), and rabbit anti-Tg were used as described previously (25). Tunicamycin was from Sigma, lipofectamine was from Invitrogen, RNeasy Mini kit was from Qiagen, Dual-Luciferase reporter assay kit was from Promega, the "cell death detection kit" was from Roche Applied Science(cat. #1544675).

Growth of MEFs—MEFs were grown routinely in DMEM containing 25 mM glucose plus 10% fetal bovine serum and 50 μM 2-mercaptoethanol. Except where otherwise stated, 2 days before experiments, cells were transferred to basal growth medium (DMEM with 5.5 mM glucose plus 10% fetal bovine serum).

Transfection—293 cells were cultured routinely in basal growth medium. Cells were transfected with plasmid DNA (encoding PERK-K618A bearing a single, C-terminal Myc tag, or similarly tagged wild-type PERK, obtained from the laboratory of Dr. D. Ron, Skirball Institute, New York University, New York, and subcloned via EcoRI and XhoI sites to the pCDNA3.1 expression vector), 2 μg per well using Lipofectamine-2000 (Invitrogen) as per the manufacturer's protocol. Thereafter, the cells were selected in DMEM containing 25 mM glucose with 10% fetal bovine serum and 50 μM 2-mercaptoethanol plus 800 μg/ml G418. G418-resistant cells were screened for the presence of Myc-tagged PERK-K618A by Western blotting and thereafter were maintained in the presence of 400 μg/ml G418. Except where otherwise stated, 2 days before experiments, all cells were transferred to basal growth medium.

Immunofluorescence—293/PERK-K618A cells (and untransfected 293 cells, used as a negative control) were fixed with 4% formaldehyde and permeabilized with 0.1% Triton X-100, blocked for 30 min at 22 °C in 5% serum in phosphate-buffered saline plus 0.02% sodium azide, and incubated for a further 30 min at 22 °C with rabbit anti-Myc (1:1000) in blocking buffer, and bound antibodies were detected with Alexa 546-tagged goat anti-rabbit secondary antibody (Jackson Immunochemicals). Digital images were captured in a standard Zeiss microscope equipped with epifluorescence optics and filters.

Metabolic Labeling—At different times after incubating 293/PERK-K618A cells and untransfected 293 cells in complete media containing tunicamycin (2.5 or 5.0 μg/ml), the cells were further incubated for 3 h blocks of time at 37 °C in the presence of 100 mCi/ml of ^{35}S-amino acid mixture (Expre^{35}S^{35}S, PerkinElmer Life Sciences) in complete high glucose DMEM containing 10% fetal bovine serum.

Following metabolic labeling, the cells were washed twice with ice-cold DMEM supplemented with an excess of cold methionine and cysteine, and then lysed by boiling directly in SDS-gel sample buffer containing 20 mM dithiothreitol. Radiolabeled proteins were resolved by SDS 8%-PAGE followed by fluorography.

Western Blotting and Measuring BiP Synthesis—After different timed exposures to tunicamycin at doses of either 2.5 or 5.0 μg/ml, 293/PERK-K618A cells and untransfected 293 cells were lysed in SDS-gel sample buffer, and 20 μg of cellular protein was resolved by SDS 8%-PAGE and electrotransferred to nitrocellulose, followed by immunoblotting for antigens described in the text. Bands were visualized by enhanced chemiluminescence.

To validate Western blotting results for BiP, BiP synthesis was followed by metabolic labeling as described above. At the conclusion of the labeling period, cells were lysed in immunoprecipitation buffer (1% Triton X-100, 25 mM Tris-HCl, 0.1 M NaCl, pH 6.8) containing a protease inhibitor mixture (26). Cell debris was cleared by low speed centrifugation, and the supernatants were immunoprecipitated with rabbit anti-BiP, washed, boiled in gel sample buffer, and analyzed by SDS 8%-PAGE and phosphorimaging.

XBP1 Production—Splicing of XBP1 mRNA in 293 cells was detected by reverse transcription-PCR. First RNA was isolated using the RNeasy Mini kit (Qiagen), reverse-transcribed from 50 ng of RNA using the One-Step RT-PCR kit (Invitrogen). For reverse transcription-PCR amplification of XBP1, the forward primer was 5′-CCTTGTAGTTGAGAACCAGG-3′, and the reverse primer was 5′-GGGGCTTGGTATATATGTGG-3′. PCR products were analyzed by agarose gel electrophoresis and visualized by ethidium bromide staining. For additional validation, XBP1 Western blotting was performed with a rabbit polyclonal anti-XBP1 antibody (Santa Cruz Biotechnology, cat. #sc-7160).

BiP-luciferase and CHOP-luciferase Assays—For Fig. 6*A* or the *upper panel* of Fig. 8*A*, 293 control and 293/PERK-K618A cells were transfected with a plasmid encoding firefly luciferase driven by ~3 kb of BiP promoter ("BiP-luciferase," the kind gift of Dr. A. Lee, University of Southern California (27)) or a plasmid encoding firefly luciferase driven by 0.9 kb of the rat CHOP promoter ("CHOP-luciferase," the kind gift of Dr. R. Kaufman, University of Michigan) and co-transfected with CMV-*Renilla* luciferase (pRL-CMV, Promega cat. #E2261). At 48 h post-transfection, the cells were lysed, and both firefly and *Renilla* luciferase activities were measured by the Dual-Luciferase reporter kit (Promega cat. #1980) with signal quantified in a Veritas luminometer (Turner Biosystems). For Fig. 5*B*, the cells

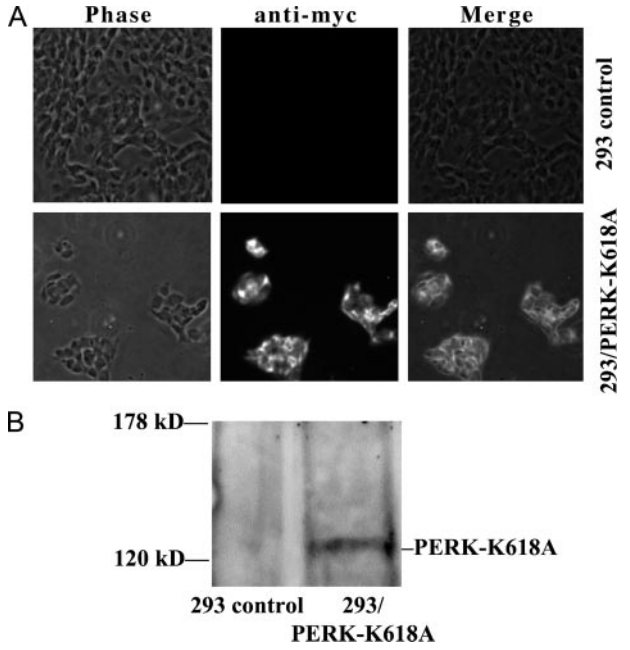

FIGURE 1. **Expression of Myc-tagged PERK-K618A in stably transfected 293 cells.** *A*, control 293 cells and 293/PERK-K618A cells were fixed, permeabilized, and stained with anti-Myc and fluorescence-conjugated secondary antibodies. All 293/PERK-K618A cells stained positively for Myc-tagged PERK-K618A. *B*, Myc Western blot of 293 control cells and 293/PERK-K618A cells.

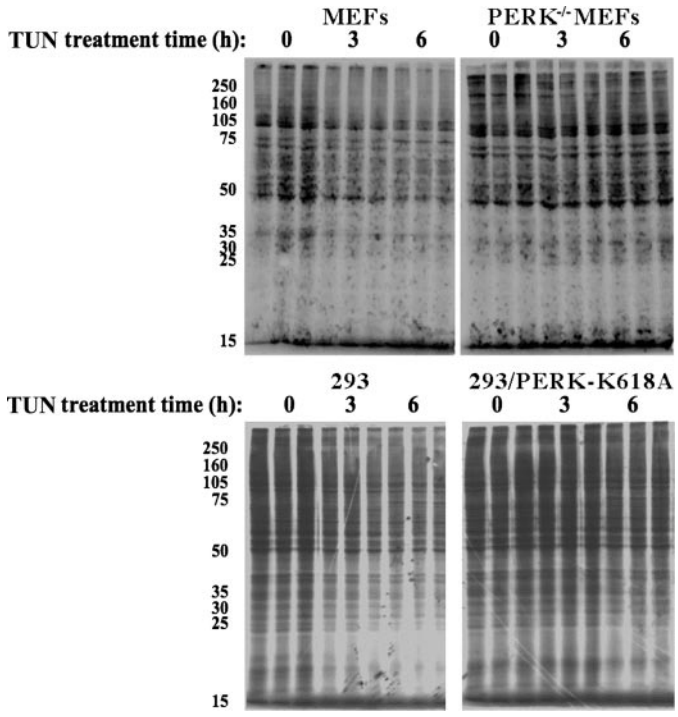

FIGURE 2. **Global protein synthesis in response to ER stress in 293/PERK-K618A cells.** To induce misfolding of unglycosylated secretory pathway proteins and ER stress, tunicamycin (*Tun*) was employed at a dose of 5.0 μg/ml (MEFs, *top panels*) or 2.5 μg/ml (293 cells, *bottom panels*) for the times indicated. Each of four sets of cells was labeled continuously, in triplicate wells, with ^{35}S-amino acids in complete medium for the last 3 h of drug treatment. Total ^{35}S-labeled cell lysate proteins, normalized to total protein, were analyzed by SDS-PAGE and autoradiography. With the exception of a few selective unidentified bands (that are likely to represent ER chaperones such as BiP), translation was suppressed to a much greater degree after onset of ER stress in control MEFs and control 293 cells than in comparable cells in which PERK function was disabled. The positions of molecular weight standards is shown at *left*.

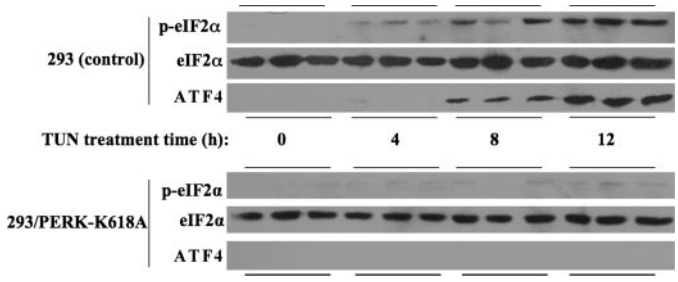

FIGURE 3. **An increase in net level of phosphoSer-51-eIF2α (p-eIF2α) and induction of ATF4 protein in response to ER stress is blocked or delayed in 293/PERK-K618A cells.** To induce misfolding of unglycosylated secretory pathway proteins and ER stress, cells were treated with tunicamycin (*TUN*, 2.5 μg/ml) for the times indicated. Lysates (normalized to total protein) from triplicate wells of control 293 cells (*top panels*) or 293/PERK-K618A cells (*bottom panels*) were resolved by SDS-PAGE and electrotransferred for Western blotting for the antigens shown. In control 293 cells, induction of ATF4 protein follows shortly after a net increase in p-eIF2α levels.

were co-transfected with BiP-luciferase and either wild-type thyroglobulin (Tg), *cog* Tg, or *rdw* Tg at a plasmid ratio of 1:5 to favor BiP-luciferase reporting from cells expressing Tg.

Cell Demise by Crystal Violet Staining—In 6-well plates, 293 and 293/PERK-K618A cells were exposed to different concentrations of tunicamycin for 48 h, washed in phosphate-buffered saline, and stained for 15 min with 0.1% (w/v) crystal violet (Sigma) in 2% ethanol, washed twice with water, with images captured by scanning as reported previously (28).

Cell Death by Sandwich ELISA Assay—To quantify death ongoing among the culture of adherent cells, culture medium was removed, and the cells were gently washed in phosphate-buffered saline, lysed in 100 μl of radioimmune precipitation assay buffer and spun at 1000 $\times$ *g* for 2 min to clear debris from the cell lysates. A sandwich ELISA assay was then employed to detect nucleosomes liberated as a consequence of apoptotic endonuclease activity, as per the manufacturer's instructions (Roche Applied Science cat. #1544675). Briefly, 100 μl of each cell lysate was applied to a pre-coated, pre-washed, pre-blocked 96-well microtiter plate containing bound mouse anti-histone antibody and incubated for 90 min at room temperature. The immune reaction was then completed by adding anti-DNA peroxidase-conjugated secondary antibody, and the peroxidase reaction was analyzed by optical density at 405 nm on a 96-well plate reader. Averages for replicate wells were normalized to protein content in parallel cell culture wells.

Cell Death by DAPI Staining—To examine death of individual transfected cells, cells growing in 6-well plates were incubated for 15 min at 37 °C with 1 ml of fresh growth medium supplemented with DAPI dilactate (Invitrogen/Molecular probes cat. #D3571). Cells were then washed very gently by removing half of the cell culture medium and replacing it with fresh medium, repeating this five times. Cells were protected from light until imaging by fluorescence microscopy in a standard Zeiss microscope equipped with epifluorescence optics and a DAPI filter set, with digital image capture. Random photographic fields were captured both by phase and fluorescence microscopy to count total cells in the field, and the fraction of DAPI-positive cells. At least three independent fields were captured for each experimental condition.

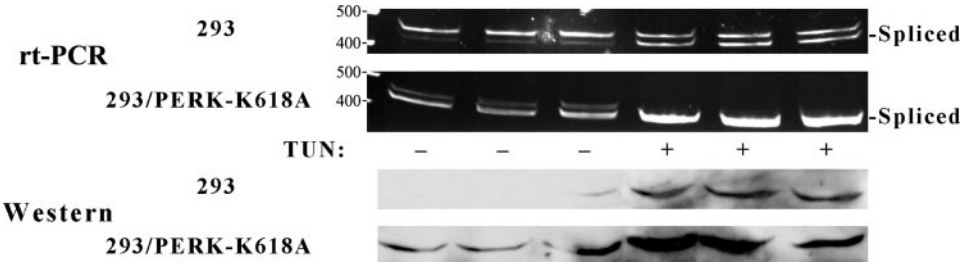

FIGURE 4. **Splice activation of XBP1 mRNA leads to up-regulated XBP1 protein expression in 293/PERK-K618A cells.** To induce misfolding of unglycosylated secretory pathway proteins and ER stress, cells were treated with 2.5 μg/ml tunicamycin (*TUN* +) for 12 h. *Upper panels*, RNA isolated from triplicate wells of control 293 cells (*293*) or 293/PERK-K618A cells was amplified by reverse transcription-PCR with the products analyzed by agarose gel electrophoresis (see "Experimental Procedures"). Both inactive (459 bp) and splice-activated forms (indicated on the figure, 415 bp) of XBP1 mRNA were recovered. *Lower panels*, triplicate lysates of the cells indicated (normalized to total protein) were analyzed by SDS-PAGE and Western blotting for XBP1 protein.

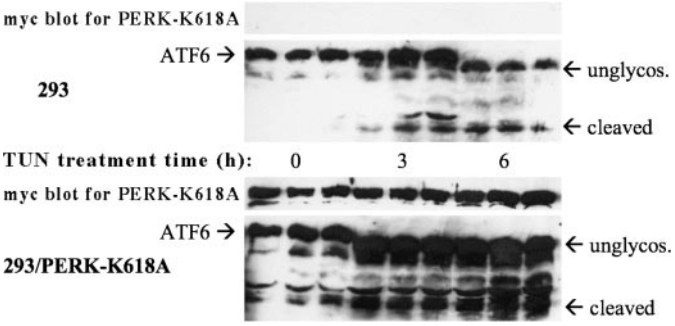

FIGURE 5. **ATF6 cleavage in response to ER stress in 293/PERK-K618A cells.** To induce misfolding of unglycosylated secretory pathway proteins and ER stress, the cells were exposed to tunicamycin (*TUN*, 5.0 μg/ml) for the times indicated. Lysates (normalized to total protein) from triplicate wells of control 293 cells (*top panels*) or 293/PERK-K618A cells (*bottom panels*) were resolved by SDS-PAGE and electrotransferred for Western blotting for ATF6 and a strip of the same membrane was blotted as a control with anti-Myc. After tunicamycin treatment, the further synthesis of ATF6 is an unglycosylated form of the protein ("*unglycos.*"), but the primary focus of the figure is the disappearance of the original glycosylated ~90-kDa ATF6 band ("*ATF6*"), which disappears more quickly in 293/PERK-K618A cells. In conjunction with this disappearance is an apparent increase in a ~50-kDa cleaved form of ATF6, whereas other bands seen in the figure may be nonspecific background.

Cell Death by Caspase 3 Activity—Cells were seeded into 24-well plates at 80% confluency. At 16 h post-seeding, triplicate wells were transfected with 500 ng/well pCMS plasmids containing either wild-type human proinsulin, proinsulin C(A7)Y, or empty vector. At 30 h post-transfection, culture plates were examined for GFP expression among the cell population before returning to the incubator. At 48 h post-transfection, cells were trypsinized (and the trypsin neutralized with fresh medium), counted in suspension, and 10^5 cells in 50 μl from each group were analyzed for activity by luminescence using the Caspase-3/7 Glo kit (Promega, Madison, WI) as per the manufacturer's instructions. Luminescence was measured in a Veritas 96-well plate luminometer.

RESULTS

Production of 293/PERK-K618A Cells—A construct encoding the dominant-negative, Myc-tagged PERK-K618A mutant (19) was transfected into 293 cells and stably transfected cells selected for G418 resistance. We found that, especially in the weeks immediately following transfection, optimal viability of the cells required addition of 50 μM 2-mercaptoethanol to the growth medium, which allowed the cells to be expanded and frozen. Immunofluorescence staining of these cells revealed that the entire population was expressing the PERK-K618A construct (Fig. 1*A*), which was also detectable by Western blotting (Fig. 1*B*).

One aspect of PERK function is, upon ER stress, to inhibit further general protein synthesis. Indeed, in MEFs from normal mice, within 3 h of treatment with tunicamycin, new synthesis of proteins was inhibited as measured by the spectrum of trichloroacetic acid-precipitable radiolabeled proteins (Fig. 2, *upper left panel*) as expected. MEFs from PERK$^{-/-}$ mice entirely lacking the PERK gene product were defective for down-regulating protein synthesis (Fig. 2, *upper right*). In control 293 cells (Fig. 2, *bottom left*), tunicamycin treatment also suppresses protein synthesis. 293/PERK-K618A cells that do not lack the PERK gene product but do express the dominant-negative PERK-K618A also exhibited deficiency in down-regulating new protein synthesis (Fig. 2, *bottom right*). These data support the notion of defective PERK kinase activity in cells expressing PERK-K618A cells (19).

PERK Activity in 293/PERK-K618A Cells—To more directly test PERK kinase activity, we examined the levels of phosphoSer-51-eIF2α in control 293 cells and PERK-K618A cells as a function of time after tunicamycin treatment. In control 293 cells, basal levels of phospho-eIF2α were low and rose steadily over 12 h of tunicamycin treatment (Fig. 3, *upper panels*). One of the selective effects of eIF2α phosphorylation is augmented translation of the ATF4 transcription factor that carries out a portion of the ER stress response (18). Indeed, in control 293 cells, ATF4 protein expression became apparent during the course of tunicamycin treatment (Fig. 3, *upper panels*). However, in 293/PERK-K618A cells treated with tunicamycin, only low levels of phospho-eIF2α (presumably phosphorylated by other kinases linked to the integrated stress response) were recovered throughout the course of the experiment, and ATF4 protein levels remained below detection (Fig. 3, *lower panels*).

Activity of Other Limbs of the Tripartite ER Stress Response in 293/PERK-K618A Cells—In addition to PERK, major ER stress signaling molecules in the membrane of the ER include Ire1 and ATF6 (29).

To directly test Ire1 ribonuclease activity, we examined the splicing of XBP1 mRNA to a shorter form leading to production of the active transcription factor (17). As shown in Fig. 4 in control 293 cells, a larger form of XBP1 mRNA predominated in the absence of added ER stress, and a new shorter form began to emerge after tunicamycin treatment (*upper panel*). By contrast in 293/PERK-K618A cells, the shorter form of XBP1 was already predominant even before imposition of added ER stress, and the intensity of this mRNA signal increased further after tunicamycin treatment (Fig. 4). These changes were also reflected at the level of translated XBP1, in which the protein

became apparent after tunicamycin treatment (Fig. 4, *lower panels*). Specifically, in 293/PERK-K618A cells XBP1 protein was already detected in the absence of added ER stress, and the intensity of this band increased further after tunicamycin treatment (Fig. 4, *bottom panel*). These data are consistent with the notion of hyperactivity of the Ire1-XBP1 system (30) in 293 cells with defective PERK activity.

The ER stress response protein ATF6 can itself be up-regulated by ER stress (14, 21). Moreover, ER stress abrogates pro-ATF6 retention within the ER, allowing the protein to migrate to the Golgi complex (15) where its cytosolic domain is cleaved to become an active nuclear transcription factor (17, 31–33). In 293 cells after treatment with 5 μg/ml tunicamycin (Fig. 5, *upper panels*), onset of cleavage of pro-ATF6 was slow, taking 6 h to achieve complete disappearance of pre-existing (glycosylated) pro-ATF6 (with appearance of the active ~50 kDa cleaved fragment as well as newly synthesized unglycosylated pro-ATF6). 293/PERK-K618A cells contained at least as much initial pro-ATF6 protein expression as control 293 cells, with all of the pre-existing (glycosylated) pro-ATF6 cleaved by 3 h after onset of ER stress, along with brisk ongoing synthesis of (unglycosylated) pro-ATF6 and apparent cleavage (Fig. 5, *lower panels*). These data also suggest robust activity of the ATF6 stress signaling system in 293/PERK-K618A cells compensating for defective PERK signaling.

Induction of Specific ER Resident Proteins and Chaperones in 293/PERK-K618A Cells—To assess the significance of the active Ire1/XBP1 and ATF6 pathways in conjunction with disabled PERK/ATF4 activation, we looked at the induction of specific ER residents of 293/PERK-K618A cells. We focused initial attention on BiP, by transiently transfecting these cells with a firefly luciferase reporter construct driven by a BiP promoter (27). When such transiently transfected cells were treated with tunicamycin to induce ER stress, BiP-luciferase expression in 293/PERK-K618A cells reproducibly lagged behind that observed in control 293 cells (Fig. 6*A*). We similarly examined the BiP response to ER stress induced by specific misfolded secretory

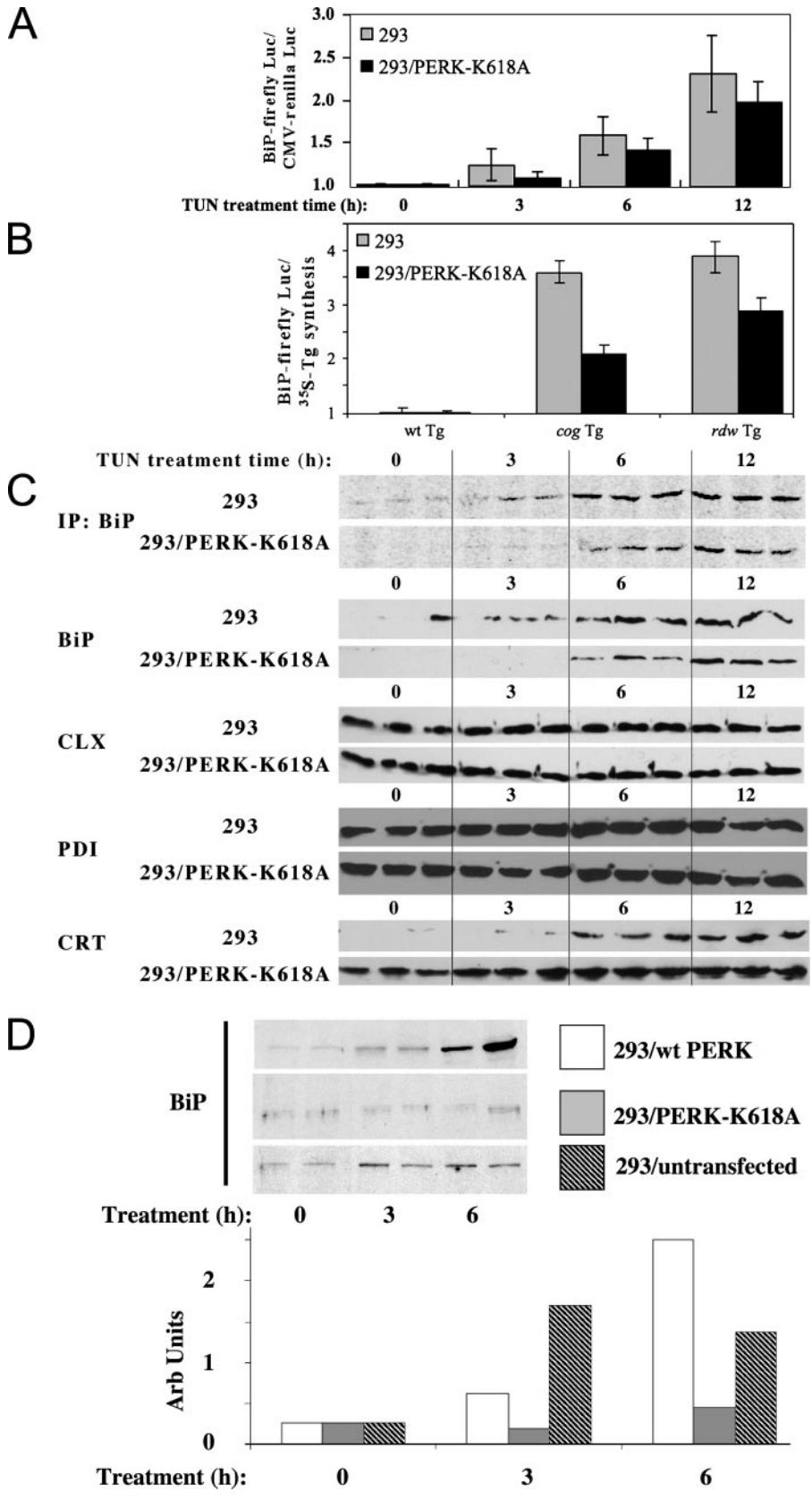

proteins. Indeed, when the cells were transfected with cDNAs encoding either *cog* Tg or *rdw* Tg (two mutant Tg alleles known to cause ER stress (25, 34)), we could normalize the BiP-luciferase response directly to the synthesis of the misfolded secretory protein. PERK/293-K618A cells were clearly deficient for BiP induction by mutant Tg (Fig. 6*B*), and the results are representative of responses in the general cell population, because transfection efficiency in these experiments was ~50% (not shown). This is >10-fold greater than what we could obtain in PERK$^{-/-}$ MEF cells (not shown).

To examine authentic endogenous BiP expression, we performed two kinds of experiments. First, we examined new BiP synthesis by metabolic labeling of cells for 3 h in the absence or presence of tunicamycin treatment for different periods of time. Confirming earlier experiments, onset of increased BiP synthesis was delayed in 293/PERK-K618A cells (Fig. 6*C*, *upper panels*). In independent experiments without radiolabeling, there was also a lag in induction of BiP protein levels by Western blotting (*second set of panels*, Fig. 6*C*). These data indicate defective BiP induction in cells with disabled PERK signaling despite the activity of Ire1/XBP1 and ATF6 pathways.

Unlike BiP, there were no major changes in calnexin or PDI levels in 293 cells treated with tunicamycin, and no major differences seen in 293/PERK-K618A cells (Fig. 6*C*). However, both "basal" and ER stress-induced calreticulin levels were higher in 293/PERK-K618A cells. The data indicate that, in 293 cells, compensatory ER stress response pathways hyperstimulate calreticulin expression even as the PERK/ATF4 pathway appears necessary for full BiP induction.

To confirm that the phenotype of 293/PERK-K618A cells did not merely reflect the overexpression of PERK in the ER, we also transiently transfected wild-type PERK in these cells. Whereas 293/PERK-K618A cells exhibited a lag in BiP protein induction after tunicamycin treatment, 293/wt PERK cells exhibited exuberant BiP induction (Fig. 6*D*). Thus, the phenotype of 293/PERK-K618A cells is not caused simply by protein overexpression within the ER membrane.

Ire1/XBP1 and ATF6 Pathways Do Not Fully Ameliorate Compromised Cell Viability in Cells with Disabled PERK Activity—PERK insufficiency is linked to ER stress-related cell death (30) accounting for multiorgan system dysfunction in PERK-deficient Wolcott-Rallison syndrome, which results in loss of pancreatic islet cells, pancreatic exocrine cells, bone cells, and presumably cells of other secretory tissues (24, 35). Using a simple crystal violet staining procedure, Harding and colleagues (30) established that MEFs from PERK$^{-/-}$ mice exhibit increased susceptibility to cell death in response to tunicamycin treatment. Using the same assay with PERK$^{-/-}$ MEFs as a positive control (Fig. 7*A*, *left*), we found similar behavior in 293/PERK-K618A cells (*panels* at *right*). Although cell death in PERK-deficient cells has been attributed to apoptosis, the crystal violet staining assay (Fig. 7*A*) essentially measures only disappearance of cells from the culture plate. To further examine cell death from ER stress, we next utilized the "apoptosome" detection kit in which cell death could be quantified by ELISA assay (see "Experimental Procedures"). As shown in Fig. 7*B*, similar to that seen in PERK$^{-/-}$ MEFs (*upper panel*), 293/PERK-K618A cells showed increased apoptosis after onset of ER stress (*lower panel*).

We next examined caspase-3 activation in response to ER stress induced by specific misfolded secretory proteins in transiently transfected cells that co-expressed cytosolic GFP from the same plasmid DNA. As shown in Fig. 7*C*, 293/PERK-K618A cells showed slightly increased caspase-3 activity in response to transfection conditions with either wild-type proinsulin or an empty expression vector but showed further caspase-3 activation in cells expressing proinsulin-C(A7)Y (also known as proinsulin bearing the *Akita* mutation (36)). Again, co-expressed GFP fluorescence proved that more than half the cells in the population were transfected (not shown).

Finally, we used DAPI dilactate as a nucleic acid stain (similar to propidium iodide), which cannot permeate the plasma membrane of healthy cells but can enter the cytoplasm and label the nuclei of dead and dying cells. Using PERK$^{-/-}$ MEFs as a positive control, cells were always killed >80% by a 48-h tunicamycin exposure (Fig. 7*D*). When restricting our analysis to GFP-positive (*i.e.* co-transfected) cells, there was a clear increase of cell death upon expression of human proinsulin bearing the C(A7)Y *Akita* mutation in PERK$^{-/-}$ MEFs *versus* that seen in control MEFs (Fig. 7*D*). There were many more GFP-positive 293/PERK-K618A cells, and these exhibited a similar cell death response to the misfolded proinsulin (~40% of cells, with 15% cell death in control 293 cells). Taken together, the data in Fig. 7 (*A–D*) confirm that PERK activity provides a cell survival advantage in the face of both general ER stress (21, 37) and ER stress caused by specific misfolded proteins.

CHOP Activation in PERK-disabled Cells—It has been unclear the extent to which cell death in PERK-deficient cells includes activation of the pro-apoptotic transcription factor, CHOP (38–40) which can be activated downstream of the phospho-eIF2α-mediated translational increase of ATF4 (20); but ATF4 is inhibited in 293/PERK-K618A cells (Fig. 3).

FIGURE 6. **Delayed BiP induction in 293/PERK-K618A cells compared with control 293 cells.** *A* and *C*, to induce misfolding of unglycosylated secretory pathway proteins and ER stress, the cells were exposed to tunicamycin (*TUN*, 2.5 μg/ml) for the times indicated. *A*, cells were co-transfected with BiP-luciferase (*firefly*), with signal normalized for transfection efficiency with *Renilla* luciferase driven by a CMV promoter ("*Renilla*"). At staggered times prior to the 48-h time point shown, cells began treatment with tunicamycin (*TUN*, 2.5 μg/ml) to induce ER stress before measuring the firefly/*Renilla* luciferase activity ratio. The data shown are the mean of two experiments (each in triplicate). *B*, cells were co-transfected with BiP-luciferase and wild-type or mutant thyroglobulin cDNAs (*cog* Tg or *rdw* Tg). At 48-h post-transfection, triplicate wells of cells were metabolically labeled for 1 h with ^{35}S-amino acids. One aliquot of each cell lysate was immunoprecipitated with anti-Tg and analyzed by SDS-PAGE and quantitative phosphorimaging. A second aliquot from the same sample was taken for luciferase activity (shown on the ordinate, normalized to Tg synthesis). *C*, *upper panel*, cells were labeled continuously, in triplicate wells, with ^{35}S-amino acids in complete medium for the last 3 h of drug treatment as in Fig. 2. Cell lysates were then immunoprecipitated with anti-BiP and analyzed by SDS-PAGE and fluorography. *Lower four sets of panels*, at different times after TUN treatment, cell lysates (20 μg of protein per lane), in triplicate, were analyzed by Western blotting for the proteins indicated (*CLX*, calnexin; *PDI*, protein disulfide isomerase; and *CRT*, calreticulin). *D*, *upper panel*, 293 cells transiently expressing wild-type PERK, or 293/PERK-K618A cells, or untransfected cells, were treated with tunicamycin (10 μg/ml) for the times indicated before Western blotting of BiP as in Fig. 6*C*. *Lower panel*, in parallel, the same lysates were blotted for β-tubulin (not shown), and the densitometry units for BiP protein divided by that for tubulin protein and ratios, in arbitrary units (*Arb Units*) prior to tunicamycin addition. The data shown are representative of three independent experiments.

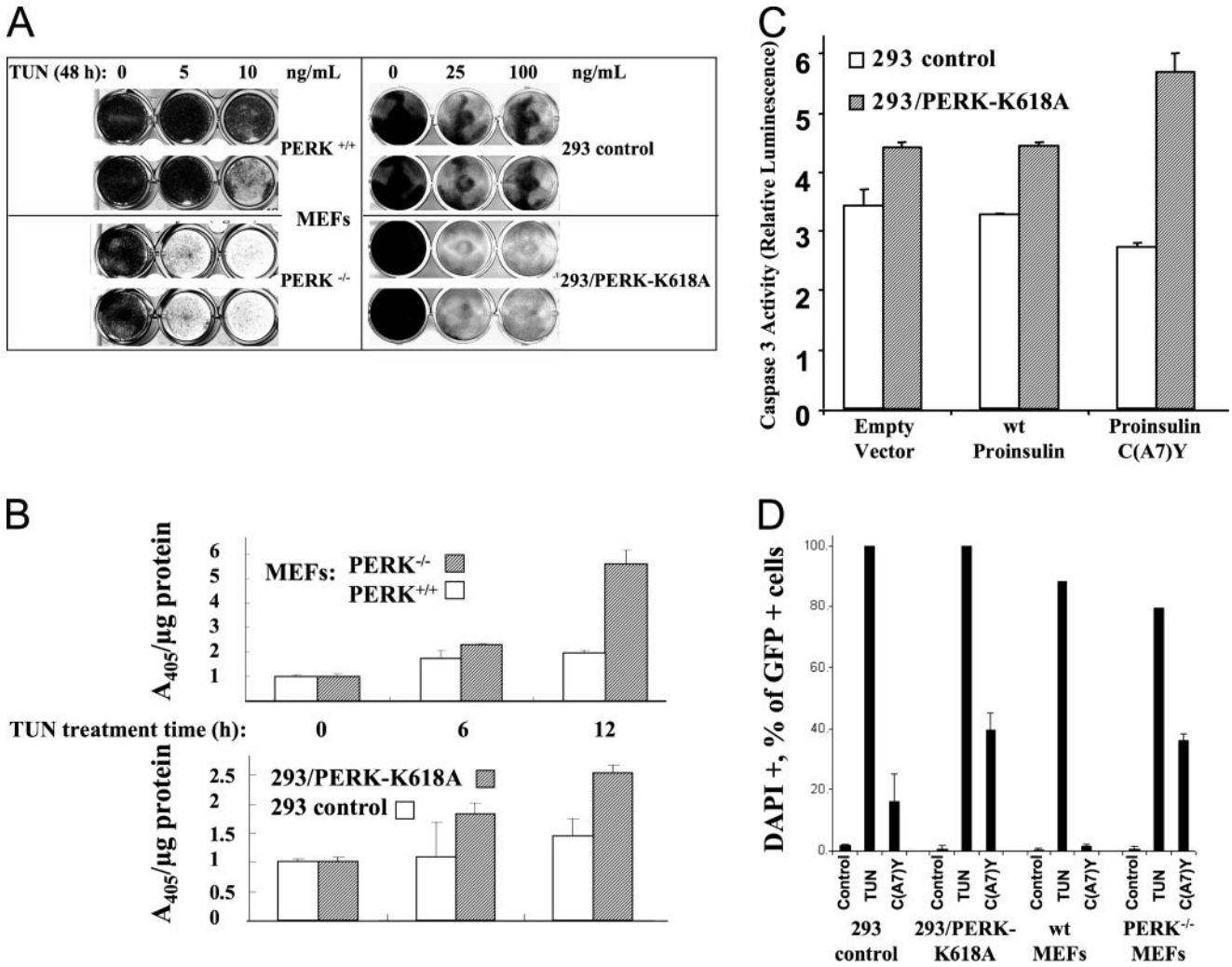

FIGURE 7. **Sensitivity of 293/PERK-K618A cells to ER stress-mediated cell death.** *A*, cells in 6-well plates were exposed (in duplicate) to tunicamycin at the doses indicated for 48 h to induce misfolding of unglycosylated secretory pathway proteins and ER stress. Remaining, surviving cells were then stained with crystal violet (see "Experimental Procedures"). Cells were lost from the cultures to a greater degree after onset of ER stress in PERK$^{-/-}$ MEFs (*left panels*) and 293/PERK-K618A cells (*right panels*). *B*, cell death measured by ELISA assay. Cells were exposed in triplicate to tunicamycin (*TUN*, 2.5 μg/ml) for the times indicated before cell lysis and ELISA assay as described under "Experimental Procedures." *C*, caspase-3 activation. Cells were exposed transfected with the plasmids indicated. At 48 h post-transfection, cell were lysed and caspase-3 measured luminometrically, in triplicate, as described under "Experimental Procedures." *D*, each of the four sets of cells indicated were either transfected with pCMS expressing cytosolic GFP and a separately encoded CMV promoter driving expression of human proinsulin bearing the *Akita*-like C(A7)Y mutation (*A7*), or put through the procedure without an insert to express any exogenous secretory protein (*no DNA*). At 48-h post-transfection, the living cultures were incubated with DAPI dilactate as described under "Experimental Procedures" and then examined by fluorescence microscopy. The percentage of green fluorescent cells (*i.e.* transfected cells) exhibiting positive nuclear staining is an estimate of dead cells exhibiting plasma membrane permeability to DAPI dilactate. As a positive control, cells were treated for 24 h with 10 μg/ml tunicamycin (*TUN*). A minimum of three different fields of cells were counted for each sample, and the fraction of DAPI-positive cells was used to generate the mean $\pm$ S.D. The data are derived from multiple fields from a single experiment, but are representative of three independent experiments. Both PERK-deficient MEFs and 293/PERK-K618A cells exhibited increased cell death ($\sim$40%) in response to expression of misfolded proinsulin.

To examine CHOP activation in PERK-disabled 293 cells, we first transiently transfected these cells with a firefly luciferase reporter construct driven by the rat CHOP promoter. When 293/PERK-K618A cells were treated with tunicamycin to induce ER stress over a 6-h period, CHOP-firefly luciferase expression clearly did not initiate as it did in control 293 cells (Fig. 8*A*, *upper panel*). We then looked over an early time course directly at authentic CHOP protein expression by Western blot and again 293/PERK-K618A cells showed a defect in time-dependent accumulation of CHOP protein (Fig. 8*A*, *bottom panel*). Because apoptosome formation in 293/PERK-K618A cells was already ongoing at 6–12 h after onset of ER stress (Fig. 7*B*), these data suggest that those 293/PERK-K618A cells dying shortly after onset of ER stress are unlikely to utilize CHOP expression (Fig. 8*A*) as an inciting mechanism.

Independent of phospho-eIF2α-mediated translational increase of ATF4, Ire1 (41) and ATF6 (33) have also been implicated in increased CHOP expression, and both are robustly active in 293/PERK-K618A cells (Figs. 4 and 5). To determine whether CHOP protein was eventually induced in these cells, experiments were extended to 24 h and 30 h, respectively. Indeed, induction of CHOP protein was detected in 293/PERK-K618A cells at 24 h after onset of ER stress and persisted at 30 h after onset of ER stress (Fig. 8*B*, *two independent experiments*). Although these data do not help to account for increased cell death within the first 12 h after

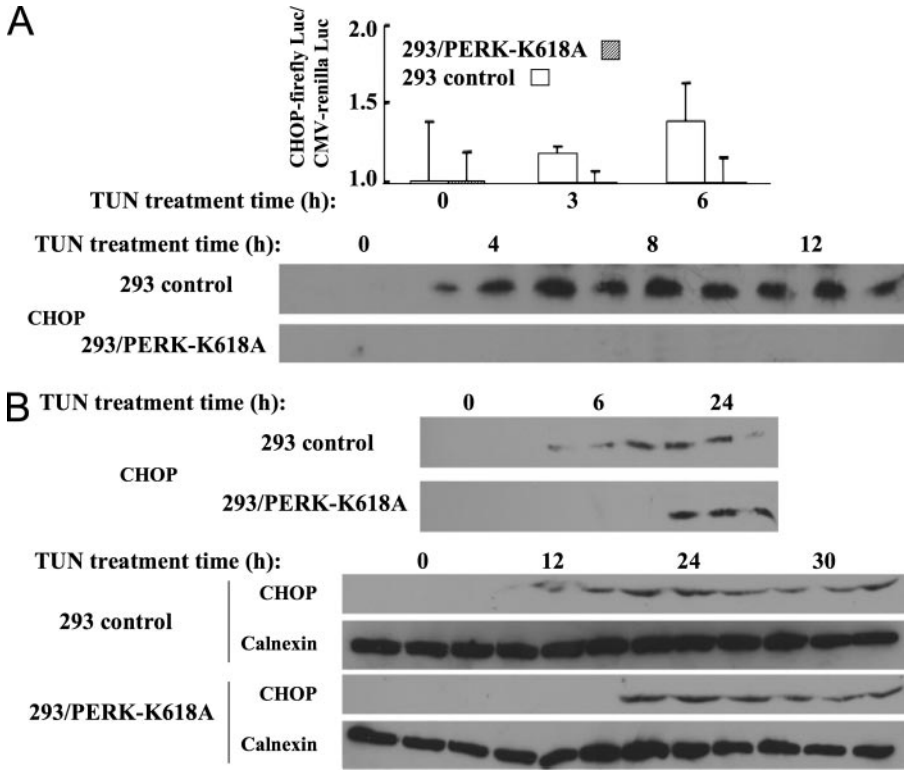

FIGURE 8. **Induction of CHOP in 293/PERK-K618A cells.** To induce misfolding of unglycosylated secretory pathway proteins and ER stress, the cells were exposed to tunicamycin (2.5 μg/ml) for the number of hours indicated. *A*, *upper panel*, cells were co-transfected with CHOP-luciferase (*firefly*), normalized for transfection efficiency with CMV-*Renilla* luciferase (*Renilla*). At 48-h post-transfection, cells began treatment with tunicamycin for the times indicated to induce ER stress before measuring the firefly/*Renilla* luciferase activity ratio. The data shown are the mean of two experiments (each in triplicate). *Lower panel*, at different times up to 12 h of TUN treatment, triplicate cell lysates, normalized to total protein, were analyzed by Western blotting for endogenous CHOP protein. Note that using either the reporter gene assay or measuring endogenous CHOP, 293/PERK-K618A cells exhibited a delayed or absence response up to 12 h after onset of ER stress. *B*, at different times of TUN treatment, triplicate cell lysates, normalized to total protein, were analyzed by Western blotting for endogenous CHOP protein. Two independent experiments are shown, and in the second experiment, immunoblotting for calnexin was included as an additional gel loading control. Note that 293/PERK-K618A cells exhibited an adequate CHOP response at 24 or more hours after onset of ER stress.

onset of ER stress (Fig. 7*B*), they certainly can account for cell death under states of chronic ER stress (Fig. 7, *A*, *C*, and *D*).

DISCUSSION

Because of difficulty in getting high transfection efficiency in MEFs, it seemed that there might be utility in generating a stable 293 cell line in which PERK was disabled yet the cells could still be readily transfected. Such an outcome might be achieved using short hairpin RNA, but previous reports have established that Myc-tagged PERK-K618A is an effective and specific dominant-negative inhibitor of PERK kinase activity (19), which is readily detected and well expressed throughout the entire population of 293/PERK-K18A cells (Fig. 1*A*). Initially we found such cells exhibited difficulty in propagation and could not be readily frozen and recovered. However, inclusion of 50 μM 2-mercaptoethanol greatly improved 293/PERK-K618A cell survival and allowed us to expand the selected population of stably transfected cells for further study. 293/PERK-K618A cells exhibit a number of features that also have been recognized in MEFs derived from PERK$^{-/-}$ mice. A schematic is presented to summarize these findings (Fig. 9).

PERK kinase activity generates phosphoSer-51-eIF2α (*middle pathway*, Fig. 9), which normally suppresses translation of most mRNAs in response to ER stress (42). However, under these conditions, 293/PERK-K618A cells do not adequately suppress new protein synthesis (Fig. 2), and this can be directly attributed to a failure to raise intracellular levels of phospho-eIF2α (Fig. 3). Another established consequence of disabling PERK is an inability of ER stress to induce ATF4 (20), and this is also observed in 293/PERK-K618A cells (Fig. 3).

Cells experiencing these defects are likely to have a survival disadvantage (18). We don't fully understand how such cells avoid apoptosis, but part of the story is likely to involve compensatory or adaptive responses (30, 43) of the remaining functional ER stress signaling pathways (*upper and lower pathways*, Fig. 9). Specifically, 293/PERK-K618A cells exhibit constitutively up-regulated splice activation of XBP1 mRNA with increased basal levels of the active transcription factor protein, and even further XBP1 mRNA splicing with higher XBP1 protein levels after ER stress (Fig. 4). Additionally, these cells abundantly express pro-ATF6 (the ~90-kDa membrane protein), and within 3 h of tunicamycin treatment, all of that pro-ATF6 has been cleaved (Fig. 5); this is an established mechanism for its conversion to an active transcription factor (17). Thus, the intriguing imbalance created by expression of PERK-K618A is a chronic *disability* of ER stress-mediated eIF2α phosphorylation (and ATF4 activation) accompanied by *hyperactivity* of Ire1/XBP1 and robust ATF6 stress signaling pathways (Fig. 9).

This imbalance sheds new light on aspects of ER chaperone regulation as well as cell survival. Consistent with previous reports (27), disabling PERK-mediated ATF4 induction causes suboptimal expression of a luciferase reporter driven by the BiP promoter in cells exposed either to tunicamycin, or, more importantly, in response to specific misfolded secretory proteins (Fig. 6, *A* and *B*). This can also be observed as suboptimal induction of radiolabeled BiP synthesis, or steady-state accumulation of BiP protein (Fig. 6*C*). These phenotypes cannot be attributed merely to membrane protein overexpression within the ER (Fig. 6*D*). Although little effect of PERK deficiency is seen on the protein levels of calnexin and PDI, 293/PERK-K618A cells actually show an overabundance of calreticulin, even prior to ER stress induction (Fig. 6*C*). There is reason to believe that calreticulin expression might be linked to the

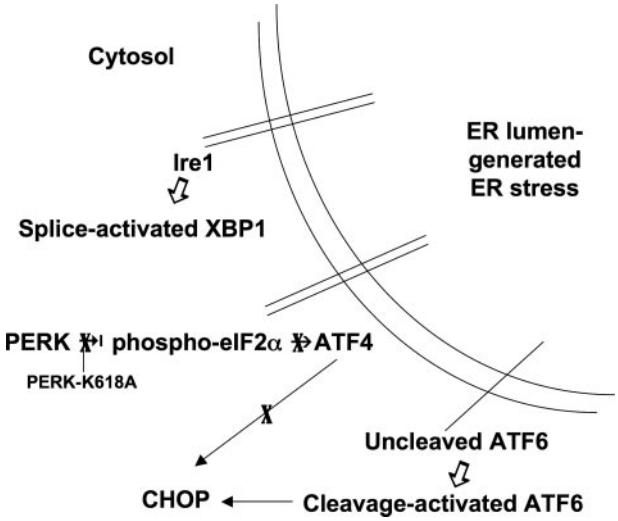

FIGURE 9. **A schematic summarizing ER stress response pathways in cells compensating for deficiency of the ER stress response kinase, PERK.** In 293/PERK-K618A cells, presence of the dominant-negative PERK mutant interferes with phosphorylation of eIF2α (*middle pathway*), causing dysregulation of protein synthesis (Fig. 2) and inhibiting induced ATF4 protein expression (Fig. 3) and its downstream induction of CHOP (Fig. 8). In such cells Ire1 (*upper pathway*) appears hyperactive in the splice activation of XBP1 mRNA and protein (Fig. 4). Likewise, ATF6 (*lower pathway*) remains robustly active in these cells (Fig. 5).

hyperactivity of XBP1 in these cells, as has been suggested in other systems (44). These data highlight selectivity of ER stress signaling pathways on the ultimate accumulation of specific ER chaperones and resident proteins.

Curiously, overexpression of calreticulin has been reported to sensitize cells to ER stress-induced apoptosis (45). Interestingly, when compared with control 293 cells, 293/PERK-K618A cells showed augmented cell death (Fig. 7*A*) that could first be detected within 6–12 h after onset of ER stress (Fig. 7*B*). CHOP has been repeatedly implicated as a key mediator of ER stress-induced cell death (38–40, 46–48) via translational up-regulation of ATF4 (20). However, this step is deficient in 293/PERK-K618A cells (Fig. 3). Moreover, in 293/PERK-K618A cells, CHOP induction clearly does not begin during the first 12 h after onset of ER stress (Fig. 8). These data strongly imply that the enhanced early cell death response to ER stress in PERK-deficient cells is mediated by mechanisms that do not involve CHOP.

This is not to say that PERK-deficient cells fail to activate CHOP; rather, they do so more slowly, because CHOP induction eventually rebounds to levels that equal those found in control cells (Fig. 8*B*). Thus, distinct early-onset and late-onset mechanisms are likely to be engaged in ER stress-mediated cell death, at least in cells with insufficient PERK kinase activity. The net effect of these mechanisms includes augmented cell death in response to specific misfolded secretory proteins, such as misfolded proinsulin (Fig. 7*C*). Cavener and colleagues (49) have recently suggested that it is primarily a failure of proliferation and differentiation of pancreatic β-cells that causes diabetes in PERK-deficient mice, and perhaps in human Wolcott-Rallison syndrome. However, our data continue to support an earlier view that insufficient PERK signaling (50), especially in response to misfolded proinsulin (51), leaves cells particularly susceptible to death from ER stress (52). There is absolutely no question that β-cell proliferation and differentiation in early life give humans (and animal models) a crucial "running start" in generating the pancreatic β-cell mass needed to maintain normal insulin secretory function; however, we believe that cell death from misfolding of proinsulin (36) (and other secretory proteins in other secretory cell types (53)) in the setting of absolute or relative PERK deficiency is an area that requires serious further investigation.

Acknowledgment—We acknowledge Lori Bash, who as an undergraduate rotation student participated in plasmid subcloning.

REFERENCES

1. Rutishauser, J., and Spiess, M. (2002) *Swiss Med. Wkly.* **132,** 211–222
2. Kim, P. S., and Arvan, P. (1998) *Endocr. Rev.* **19,** 173–202
3. Wu, Y., Swulius, M. T., Moremen, K. W., and Sifers, R. N. (2003) *Proc. Natl. Acad. Sci. U. S. A.* **100,** 8229–8234
4. Ellgaard, L., and Helenius, A. (2003) *Nat. Rev. Mol. Cell. Biol.* **4,** 181–191
5. Kostova, Z., and Wolf, D. H. (2003) *EMBO J.* **22,** 2309–2317
6. Meusser, B., Hirsch, C., Jarosch, E., and Sommer, T. (2005) *Nat. Cell Biol.* **7,** 766–772
7. Sekijima, Y., Wiseman, R. L., Matteson, J., Hammarström, P., Miller, S. R., Sawkar, A. R., Balch, W. E., and Kelly, J. W. (2005) *Cell* **121,** 73–85
8. Chen, Y., Bellamy, W. P., Seabra, M. C., Field, M. C., and Ali, B. R. (2005) *Hum. Mol. Genet.* **14,** 2559–2569
9. Marciniak, S. J., and Ron, D. (2006) *Physiol. Rev.* **86,** 1133–1149
10. Chapman, R., Sidrauski, C., and Walter, P. (1998) *Annu. Rev. Cell Dev. Biol.* **14,** 459–485
11. Calfon, M., Zeng, H., Urano, F., Till, J. H., Hubbard, S. R., Harding, H. P., Clark, S. G., and Ron, D. (2002) *Nature* **415,** 92–96
12. Sidrauski, C., and Walter, P. (1997) *Cell* **90,** 1031–1039
13. Travers, K. J., Patil, C. K., Wodicka, L., Lockhart, D. J., Weissman, J. S., and Walter, P. (2000) *Cell* **101,** 249–258
14. Yoshida, H., Matsui, T., Hosokawa, N., Kaufman, R. J., Nagata, K., and Mori, K. (2003) *Dev. Cell* **4,** 265–271
15. Shen, J., Chen, X., Hendershot, L., and Prywes, R. (2002) *Dev. Cell* **3,** 99–111
16. Yoshida, H., Matsui, T., Yamamoto, A., Okada, T., and Mori, K. (2001) *Cell* **107,** 881–891
17. Lee, K., Tirasophon, W., Shen, X., Michalak, M., Prywes, R., Okada, T., Yoshida, H., Mori, K., and Kaufman, R. J. (2002) *Genes Dev.* **16,** 452–466
18. Harding, H. P., Zhang, Y., Zeng, H., Novoa, I., Lu, P. D., Calfon, M., Sadri, N., Yun, C., Popko, B., Paules, R., Stojdl, D. F., Bell, J. C., Hettmann, T., Leiden, J. M., and Ron, D. (2003) *Mol. Cell.* **11,** 619–633
19. Harding, H. P., Zhang, Y., and Ron, D. (1999) *Nature* **397,** 271–274
20. Harding, H. P., Novoa, I., Zhang, Y., Zeng, H., Wek, R., Schapira, M., and Ron, D. (2000) *Mol. Cell* **6,** 1099–1108
21. Lu, P. D., Jousse, C., Marciniak, S. J., Zhang, Y., Novoa, I., Scheuner, D., Kaufman, R. J., Ron, D., and Harding, H. P. (2004) *EMBO J.* **23,** 169–179
22. Bertolotti, A., Zhang, Y., Hendershot, L. M., Harding, H. P., and Ron, D. (2000) *Nat. Cell Biol.* **2,** 326–332
23. Ma, K., Vattem, K. M., and Wek, R. C. (2002) *J. Biol. Chem.* **277,** 18728–18735
24. Zhang, P., McGrath, B., Li, S., Frank, A., Zambito, F., Reinert, J., Gannon, M., Ma, K., McNaughton, K., and Cavener, D. R. (2002) *Mol. Cell. Biol.* **22,** 3864–3874
25. Kim, P. S., Kwon, O.-Y., and Arvan, P. (1996) *J. Cell Biol.* **133,** 517–527
26. Caldwell, S. R., Hill, K. J., and Cooper, A. A. (2001) *J. Biol. Chem.* **276,** 23296–23303
27. Luo, S., Baumeister, P., Yang, S., Abcouwer, S. F., and Lee, A. S. (2003) *J. Biol. Chem.* **278,** 37375–37385
28. Ramos-Castañeda, J., Park, Y.-n., Liu, M., Hauser, K., Rudolph, H., Shull, G. E., Jonkman, M. F., Mori, K., Ikeda, S., Ogawa, H., and Arvan, P. (2005) *J. Biol. Chem.* **280,** 9467–9473

29. Schroder, M., and Kaufman, R. J. (2005) *Annu. Rev. Biochem.* **74,** 739–789
30. Harding, H. P., Zhang, Y., Bertolotti, A., Zeng, H., and Ron, D. (2000) *Mol. Cell* **5,** 897–904
31. Haze, K., Yoshida, H., Yanagi, H., Yura, T., and Mori, K. (1999) *MBC* **10,** 3787–3799
32. Ye, J., Rawson, R. B., Komuro, R., Chen, X., Dave, U. P., Prywes, R., Brown, M. S., and Goldstein, J. L. (2000) *Mol. Cell* **6,** 1355–1364
33. Yoshida, H., Okada, T., Haze, K., Yanagi, H., Yura, T., Negishi, M., and Mori, K. (2000) *Mol. Cell. Biol.* **20,** 6755–6767
34. Menon, S., Lee, J., Abplanalp, W. A., Yoo, S. E., Agui, T., Furudate, S., Kim, P. S., and Arvan, P. (2007) *J. Biol. Chem.* **282,** 6183–6191
35. Li, Y., Iida, K., O'Neil, J., Zhang, P., Li, S., Frank, A., Gabai, A., Zambito, F., Liang, S. H., Rosen, C. J., and Cavener, D. R. (2003) *Endocrinology* **144,** 3505–3513
36. Liu, M., Hodish, I., Rhodes, C. J., and Arvan, P. (2007) *Proc. Natl. Acad. Sci. U. S. A.* **104,** 15841–15846
37. Jiang, H. Y., Wek, S. A., McGrath, B. C., Scheuner, D., Kaufman, R. J., Cavener, D. R., and Wek, R. C. (2003) *Mol. Cell. Biol.* **23,** 5651–5663
38. Wang, X. Z., Lawson, B., Brewer, J. W., Zinszner, H., Sanjay, A., Mi, L. J., Boorstein, R., Kreibich, G., Hendershot, L. M., and Ron, D. (1996) *Mol. Cell. Biol.* **16,** 4273–4280
39. Zinszner, H., Kuroda, M., Wang, X., Batchvarova, N., Lightfoot, R. T., Remotti, H., Stevens, J. L., and Ron, D. (1998) *Genes Dev.* **12,** 982–995
40. Oyadomari, S., Koizumi, A., Takeda, K., Gotoh, T., Akira, S., Araki, E., and Mori, M. (2002) *J. Clin. Invest.* **109,** 525–532
41. Wang, X. Z., Harding, H. P., Zhang, Y., Jolicoeur, E. M., Kuroda, M., and Ron, D. (1998) *EMBO J.* **17,** 5708–5717
42. Scheuner, D., Song, B., McEwen, E., Liu, C., Laybutt, R., Gillespie, P., Saunders, T., Bonner-Weir, S., and Kaufman, R. J. (2001) *Mol. Cell* **7,** 1165–1176
43. Rutkowski, D. T., Arnold, S. M., Miller, C. N., Wu, J., Li, J., Gunnison, K. M., Mori, K., Sadighi Akha, A. A., Raden, D., and Kaufman, R. J. (2006) *PLoS Biol* **4,** e374
44. Lee, D., Singaravelu, G., Park, B. J., and Ahnn, J. (2007) *J. Mol. Biol.* **372,** 331–340
45. Nakamura, K., Bossy-Wetzel, E., Burns, K., Fadel, M. P., Lozyk, M., Goping, I. S., Opas, M., Bleackley, R. C., Green, D. R., and Michalak, M. (2000) *J. Cell Biol.* **150,** 731–740
46. Murphy, T. C., Woods, N. R., and Dickson, A. J. (2001) *Biotechnol. Bioeng.* **75,** 621–629
47. Oyadomari, S., Takeda, K., Takiguchi, M., Gotoh, T., Matsumoto, M., Wada, I., Akira, S., Araki, E., and Mori, M. (2001) *Proc. Natl. Acad. Sci. U. S. A.* **98,** 10845–10850
48. Gotoh, T., Oyadomari, S., Mori, K., and Mori, M. (2002) *J. Biol. Chem.* **277,** 12343–12350
49. Zhang, W., Feng, D., Li, Y., Iida, K., McGrath, B., and Cavener, D. R. (2006) *Cell Metab.* **4,** 491–497
50. Harding, H. P., Zeng, H., Zhang, Y., Jungries, R., Chung, P., Plesken, H., Sabatini, D. D., and Ron, D. (2001) *Mol. Cell* **7,** 1153–1163
51. Liu, M., Li, Y., Cavener, D., and Arvan, P. (2005) *J. Biol. Chem.* **280,** 13209–13212
52. Ron, D. (2002) *J. Clin. Invest.* **109,** 443–445
53. Baryshev, M., Sargsyan, E., Wallin, G., Lejnieks, A., Furudate, S., Hishinuma, A., and Mkrtchian, S. (2004) *J. Mol. Endocrinol.* **32,** 903–920